

Geometry of River Networks I: Scaling, Fluctuations, and Deviations

Peter Sheridan Dodds[†]

*Department of Mathematics and Department of Earth, Atmospheric and Planetary Sciences,
Massachusetts Institute of Technology, Cambridge, MA 02139.*

Daniel H. Rothman[‡]

*Department of Earth, Atmospheric and Planetary Sciences,
Massachusetts Institute of Technology, Cambridge, MA 02139.*

(Dated: October 30, 2018)

This article is the first in a series of three papers investigating the detailed geometry of river networks. Branching networks are a universal structure employed in the distribution and collection of material. Large-scale river networks mark an important class of two-dimensional branching networks, being not only of intrinsic interest but also a pervasive natural phenomenon. In the description of river network structure, scaling laws are uniformly observed. Reported values of scaling exponents vary suggesting that no unique set of scaling exponents exists. To improve this current understanding of scaling in river networks and to provide a fuller description of branching network structure, here we report a theoretical and empirical study of fluctuations about and deviations from scaling. We examine data for continent-scale river networks such as the Mississippi and the Amazon and draw inspiration from a simple model of directed, random networks. We center our investigations on the scaling of the length of sub-basin's dominant stream with its area, a characterization of basin shape known as Hack's law. We generalize this relationship to a joint probability density and provide observations and explanations of deviations from scaling. We show that fluctuations about scaling are substantial and grow with system size. We find strong deviations from scaling at small scales which can be explained by the existence of linear network structure. At intermediate scales, we find slow drifts in exponent values indicating that scaling is only approximately obeyed and that universality remains indeterminate. At large scales, we observe a breakdown in scaling due to decreasing sample space and correlations with overall basin shape. The extent of approximate scaling is significantly restricted by these deviations and will not be improved by increases in network resolution.

PACS numbers: 64.60.Ht, 92.40.Fb, 92.40.Gc, 68.70.+w

I. INTRODUCTION

Networks are intrinsic to a vast number of complex forms observed in the natural and man-made world. Networks repeatedly arise in the distribution and sharing of information, stresses and materials. Complex networks give rise to interesting mathematical and physical properties as observed in the Internet [1], the “small-world” phenomenon [2], the cardiovascular system [3], force chains in granular media [4], and the wiring of the brain [5].

Branching, hierarchical geometries make up an important subclass of all networks. Our present investigations concern the paradigmatic example of river networks. The study of river networks, though more general in application, is an integral part of geomorphology, the theory of earth surface processes and form. Furthermore, river networks are held to be natural exemplars of allometry, i.e., how the dimensions of different parts of a structure scale or grow with respect to each other [6, 7, 8, 9, 10]. The shapes of drainage basins, for example, are reported to

elongate with increasing basin size [11, 12, 13].

At present, there is no generally accepted theory explaining the origin of this allometric scaling. The fundamental problem is that an equation of motion for erosion, formulated from first principles, is lacking. The situation is somewhat analogous to issues surrounding the description of the dynamics of granular media [14, 15], noting that erosion is arguably far more complex. Nevertheless, a number of erosion equations have been proposed ranging from deterministic [16, 17, 18, 19] to stochastic theories [20, 21, 22, 23, 24, 25]. Each of these models attempts to describe how eroding surfaces evolve dynamically. In addition, various heuristic models of both surface and network evolution also exist. Examples include simple lattice-based models of erosion [17, 26, 27, 28], an analogy to invasion percolation [29], the use of optimality principles and self-organized criticality [7, 30, 31], and even uncorrelated random networks [10, 32, 33]. Since river networks are an essential feature of eroding landscapes, any appropriate theory of erosion must yield surfaces with network

structures comparable to that of the real world. However, no model of eroding landscapes or even simply of network evolution unambiguously reproduces the wide range of scaling behavior reported for real river networks.

A considerable problem facing these theories and models is that the values of scaling exponents for river network scaling laws are not precisely known. One of the issues we address in this work is universality [10, 12]. Do the scaling exponents of all river networks belong to a unique universality class or are there a set of classes obtained for various geomorphological conditions? For example, theoretical models suggest a variety of exponent values for networks that are directed versus non-directed, created on landscapes with heterogeneous versus homogeneous erosivity and so on [10, 34, 35]. Clearly, refined measurements of scaling exponents are imperative if we are to be sure of any network belonging to a particular universality class. Moreover, given that there is no accepted theory derivable from simple physics, more detailed phenomenological studies are required.

Motivated by this situation, we perform here a detailed investigation of the scaling properties of river networks. We analytically characterize fluctuations about scaling showing that they grow with system size. We also report significant and ubiquitous deviations from scaling in real river networks. This implies surprisingly strong restrictions on the parameter regimes where scaling holds and cautions against measurements of exponents that ignore such limitations. In the case of the Mississippi basin, for example, we find that although our study region span four orders of magnitude in length, scaling may be deemed valid over no more than 1.5 orders of magnitude. Furthermore, we repeatedly find the scaling within these bounds to be only approximate and that no exact, single exponent can be deduced. We show that scaling breaks down at small scales due to the presence of linear basins and at large scales due to the inherent discreteness of network structure and correlations with overall basin shape. Significantly, this latter correlation imprints upon river network structure the effects and history of geology.

This paper is the first of a series of three on river-network geometry. Having addressed scaling laws in the present work, we proceed in second and third articles [36, 37] to consider river network structure at a more detailed level. In [36] we examine the statistics of the “building blocks” of river networks, i.e., segments of streams and sub-networks. In particular, we analytically connect distributions of various kinds of stream length. Part of this material is employed in the present article and is a direct generalization of Horton’s laws [38, 39]. In the third article [37], we proceed from the findings of [36] to characterize how these building blocks fit together. Central to this last work is the study of the frequency and spatial distributions of tributary branches along the length of a stream and is itself a generalization of the descriptive picture of Tokunaga [40, 41, 42].

II. BASIN ALLOMETRY

A Hack’s law

In addressing these broader issues of scaling in branching networks, we set as our goal to understand the river network scaling relationship between basin area a and the length l of a basin’s main stream:

$$l \propto a^h. \quad (1)$$

Known as Hack’s law [11], this relation is central to the study of scaling in river networks [12, 39]. Hack’s exponent h is empirically found to lie in the range from 0.5 to 0.7 [11, 12, 13, 43, 44, 45, 46, 47, 48]. Here, we postulate a generalized form of Hack’s law that shows good agreement with data from real world networks.

We focus on Hack’s law because of its intrinsic interest and also because many interrelationships between a large number of scaling laws are known and only a small subset are understood to be independent [12, 39]. Thus, our results for Hack’s law will be in principle extendable to other scaling laws. With this in mind, we will also discuss probability densities of stream length and drainage area.

Hack’s law is stated rather loosely in equation (1) and implicitly involves some type of averaging which needs to be made explicit. It is most usually considered to be the relationship between *mean* main stream length and drainage area, i.e.,

$$\langle l \rangle \propto a^h. \quad (2)$$

Here, $\langle \cdot \rangle$ denotes ensemble average and $\langle l \rangle = \langle l(a) \rangle$ is the mean main stream length of all basins of area a . Typically, one performs regression analysis on $\log \langle l \rangle$ against $\log a$ to obtain the exponent h .

B Fluctuations and deviations

In seeking to understand Hack’s law, we are naturally led to wonder about the underlying distribution that gives rise to this mean relationship. By considering fluctuations, we begin to see Hack’s law as an expression of basin morphology. What shapes of basins characterized by (a, l) are possible and with what probability do they occur?

An important point here is that Hack’s law does not exactly specify basin shapes. An additional connection to Euclidean dimensions of the basin is required. We may think of a basin’s longitudinal length L_{\parallel} and its width L_{\perp} . The main stream length l is reported to scale with L_{\parallel} as

$$l \propto L_{\parallel}^d, \quad (3)$$

where typically $1.0 \lesssim d \lesssim 1.1$, [12, 50]. Hence, we have $a \propto l^{1/h} \propto L_{\parallel}^{d/h}$. All other relevant scaling laws exponents can be related to the pair of exponents (d, h) which

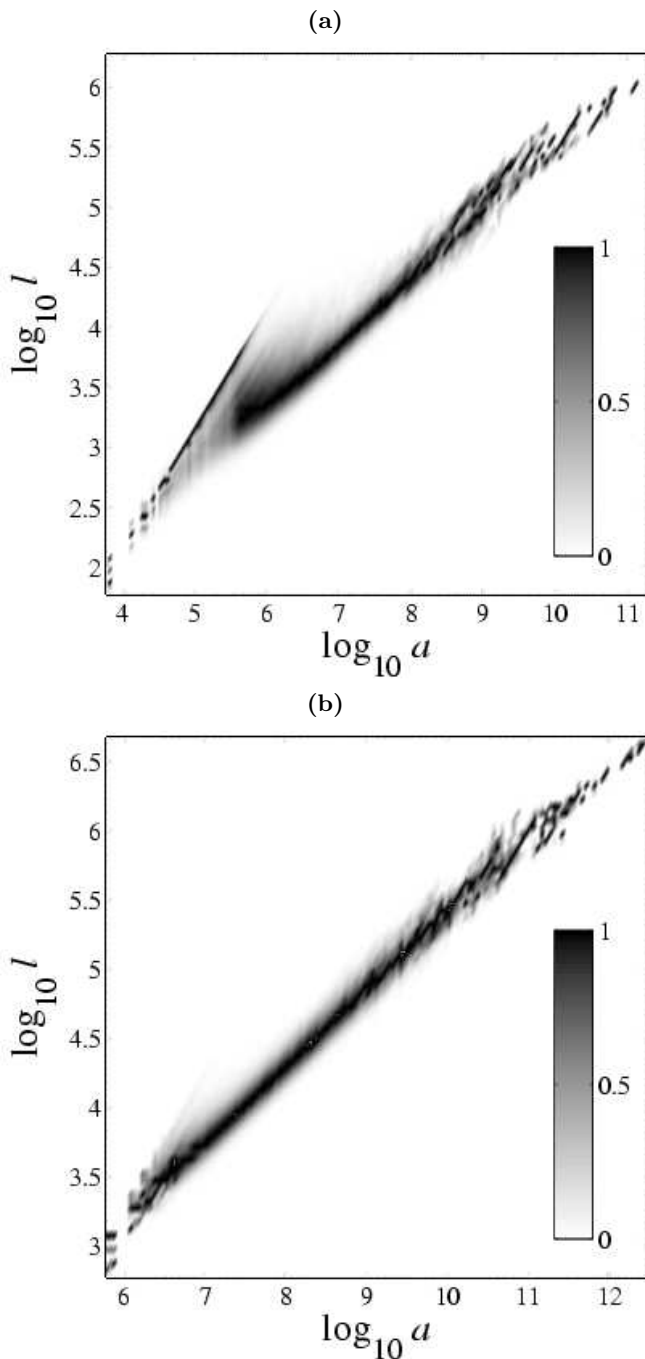


FIG. 1: The Full Hack distribution for the Kansas, (a), and Mississippi, (b), river basins. For each value of a , the distribution has been normalized along the l direction by $\max_l P(a, l)$ [49].

therefore characterize the universality class of a river network [10, 39]. If $d/h = 2$ we have that basins are self-similar whereas if $d/h < 2$, we have that basins are elongating. So, while Hack’s law gives a sense of basin allometry, the fractal properties of main stream lengths need

also be known in order to properly quantify the scaling of basin shape.

In addition to fluctuations, complementary insights are provided by the observation and understanding of deviations from scaling. We are thus interested in discerning the regularities and quirks of the joint probability distribution $P(a, l)$. We will refer to $P(a, l)$ as the *Hack distribution*.

Hack distributions for the Kansas river basin and the Mississippi river basin are given in Figures 1(a) and 1(b). Fluctuations about and deviations from scaling are immediately evident for the Kansas and to a lesser extent for the Mississippi. The first section of the paper will propose and derive analytic forms for the Hack distribution under the assumption of uniform scaling with no deviations. Here, as well as in the following two papers of this series [36, 37], we will motivate our results with a random network model originally due to Scheidegger [33].

We then expand our discussion to consider deviations from exact scaling. In the case of the Kansas river, a striking example of deviations from scaling is the linear branch separated from the body of the main distribution shown in Figure 1(a). This feature is less prominent in the lower resolution Mississippi data. Note that this linear branch is not an artifact of the measurement technique or data set used. This will be explained in our discussion of deviations at small scales in the paper’s second section.

We then consider the more subtle deviations associated with intermediate scales. At first inspection, the scaling appears to be robust. However, we find gradual drifts in “exponents” that prevent us from identifying a precise value of h and hence a corresponding universality class.

Both distributions also show breakdowns in scaling for large areas and stream lengths and this is addressed in the final part of our section on deviations. The reason for such deviations is partly due to the decrease in number of samples and hence self-averaging, as area and stream lengths are increased. However, we will show that the direction of the deviations depends on the overall basin shape. We will quantify the extent to which such deviations can occur and the effect that they have on measurements of Hack’s exponent h .

Throughout the paper, we will return to the Hack distributions for the Kansas and the Mississippi rivers as well as data obtained for the Amazon, the Nile and the Congo rivers.

III. FLUCTUATIONS: AN ANALYTIC FORM FOR THE HACK DISTRIBUTION

To provide some insight into the nature of the underlying Hack distribution, we present a line of reasoning that will build up from Hack’s law to a scaling form of $P(a, l)$. First let us assume for the present discussion of

fluctuations that an exact form of Hack's law holds:

$$\langle l \rangle = \theta a^h \quad (4)$$

where we have introduced the coefficient θ which we discuss fully later on. Now, since Hack's law is a power law, it is reasonable to postulate a generalization of the form

$$P(l|a) = \frac{1}{a^h} F_l \left(\frac{l}{a^h} \right). \quad (5)$$

The prefactor $1/a^h$ provides the correct normalization and F_l is the "scaling function" we hope to understand. The above will be our notation for all conditional probabilities. Implicit in equation (5) is the assumption that all moments and the distribution itself also scale. For example, the q th moment of $P(l|a)$ is

$$\langle l^q(a) \rangle \propto a^{qh}, \quad (6)$$

which implies

$$\langle l^q(a) \rangle = k^{-qh} \langle l^q(ak) \rangle. \quad (7)$$

where $k \in \mathbb{R}$. Also, for the distribution $P(l|a)$ it follows from equation (5) that

$$k^h P(lk^h | ak) = \frac{k^h}{a^h k^h} F_l \left(\frac{lk^h}{a^h k^h} \right) = P(l|a). \quad (8)$$

We note that previous investigations of Hack's law [12, 13] consider the generalization in equation (5). Rigon *et al.* [48] also examine the behavior of the moments of the distribution $P(l|a)$ for real networks. Here, we will go further to characterize the full distribution $P(a, l)$ as well as both $P(l|a)$ and $P(a|l)$. Along these lines, Rigon *et al.* [13] suggest that the function $F_l(x)$ is a "finite-size" scaling function analogous to those found in statistical mechanics, i.e.: $F_l(x) \rightarrow 0$ as $x \rightarrow \infty$ and $F_l(x) \rightarrow c$ as $x \rightarrow 0$. However, as we will detail below, the restrictions on $F_l(x)$ can be made stronger and we will postulate a simple Gaussian form. More generally, $F_l(x)$ should be a unimodal distribution that is non-zero for an interval $[x_1, x_2]$ where $x_1 > 0$. This is so because for any given fixed basin area a , there is a minimum and maximum l beyond which no basin exists. This is also clear upon inspection of Figures 1(a) and 1(b).

We observe that neither drainage area nor main stream length possess any obvious features so as to be deemed the independent variable. Hence, we can also view Hack's law as its inversion $\langle a \rangle \propto l^{1/h}$. Note that the constant of proportionality is not necessarily $\theta^{1/h}$ and is dependent on the nature of the full Hack distribution. We thus have another scaling ansatz as per equation (5)

$$P(a|l) = 1/l^{1/h} F_a(a/l^{1/h}). \quad (9)$$

The conditional probabilities $P(l|a)$ and $P(a|l)$ are related to the joint probability distribution as

$$P(a, l) = P(a)P(l|a) = P(l)P(a|l), \quad (10)$$

where $P(l)$ and $P(a)$ are the probability densities of main stream length and area. These distributions are in turn observed to be power laws both in real world networks and models [7, 51, 52]:

$$P(a) \sim N_a a^{-\tau} \quad \text{and} \quad P(l) \sim N_l l^{-\gamma}. \quad (11)$$

where N_a and N_l are appropriate prefactors and the tilde indicates asymptotic agreement between both sides for large values of the argument. Furthermore, the exponents τ and γ are related to Hack's exponent h via the scaling relations [12, 39]

$$\tau = 2 - h \quad \text{and} \quad \gamma = 1/h. \quad (12)$$

Equations (5), (9), (10), (11), and (12) combine to give us two forms for $P(a, l)$,

$$P(a, l) = 1/a^2 F(l/a^h) = 1/l^{2/h} G(a/l^{1/h}), \quad (13)$$

where $x^{-2}F(x^{-h}) = G(x)$ and, equivalently, $F(y) = y^{-2}G(y^{-1/h})$.

IV. RANDOM DIRECTED NETWORKS

We will use results from the Scheidegger model [33] to motivate the forms of these distributions. In doing so, we will also connect with some problems in the theory of random walks.

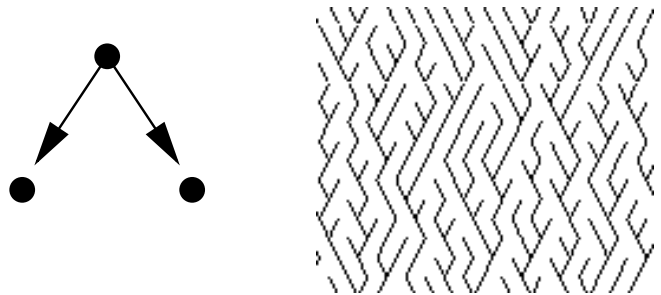


FIG. 2: Scheidegger's model of random, directed networks. Flow is down the page and at each site, stream flow is randomly chosen to be in one of the two downward diagonals. Stream paths and basin boundaries are thus discrete random walks.

Scheidegger's model of river networks is defined on a triangular lattice as indicated by Figure 2. Flow in the figure is directed down the page. At each site, the stream flow direction is randomly chosen between the two diagonal directions shown. Periodic boundary conditions are applied in all of our simulations. Each site locally drains an area of α^2 , where the lattice unit α is the distance between neighboring sites, and each segment of stream has a length α . For simplicity, we will take α to be unity. We note that connections exist between the Scheidegger model and models of particle aggregation [51, 53],

Abelian sandpiles [54, 55, 56] and limiting cases of force chain models in granular media [4].

Since Scheidegger's model is based on random flow directions, the Hack distributions have simple interpretations. The boundaries of drainage basins in the model are random walks. Understanding Hack's law therefore amounts to understanding the first collision time of two random walks that share the same origin in one dimension. If we subtract the graph of one walk from the other, we see that the latter problem is itself equivalent to the first return problem of random walks [57].

Many facets of the first return problem are well understood. In particular, the probability of n , the number of steps taken by a random walk until it first returns to the origin, is asymptotically given by

$$P(n) \sim \frac{1}{\sqrt{2\pi}} n^{-3/2}. \quad (14)$$

But this number of steps is also the length of the basin l . Therefore, we have

$$P(l) \sim \frac{2}{\pi} l^{-3/2}, \quad (15)$$

where because we are considering the difference of two walks, we use $P(l) = P(n/2)|_{n=l}$. Also, we have found the prefactor $N_l = 2/\pi$.

We thus have that $\gamma = 3/2$ for the Scheidegger model. The scaling relations of equation (12) then give $h = 2/3$ and $\tau = 4/3$. The value of h is also readily obtained by noting that the typical area of a basin of length l is $a \propto l \cdot l^{1/2} = l^{3/2} = l^{1/h}$ since the boundaries are random walks.

V. AREA-LENGTH DISTRIBUTION FOR RANDOM, DIRECTED NETWORKS

Something that is less well studied is the joint distribution of the area enclosed by a random walk and the number of steps to its first return. In terms of the Scheidegger model, this is precisely the Hack distribution.

We motivate some general results based on observations of the Scheidegger model. Figure 3 shows the normalized distributions $P(al^{-3/2})$ and $P(la^{-2/3})$ as derived from simulations of the model. Given the scaling ansatzes for $P(l|a)$ and $P(a|l)$ in equations (5) and (9), we see that $P(y=la^{-2/3}) = F_l(y)$ and $P(x=al^{-3/2}) = F_a(x)$.

Note that we have already used Hack's law for the Scheidegger model with $h = 2/3$ to obtain these distributions. The results are for ten realizations of the model on a 10^4 by 10^4 lattice, taking 10^7 samples from each of the ten instances. For $P(a|l)$, only sites where $l \geq 100$ were taken, and similarly, for $P(l|a)$, only sites where $a \geq 500$ were included in the histogram.

We postulate that the distribution $P(y = la^{-2/3})$ is a Gaussian having the form

$$P(l|a) = \frac{1}{\sqrt{2\pi a^{2/3} \eta}} \exp\{-(la^{-2/3} - \theta)^2 / 2\eta^2\} \quad (16)$$

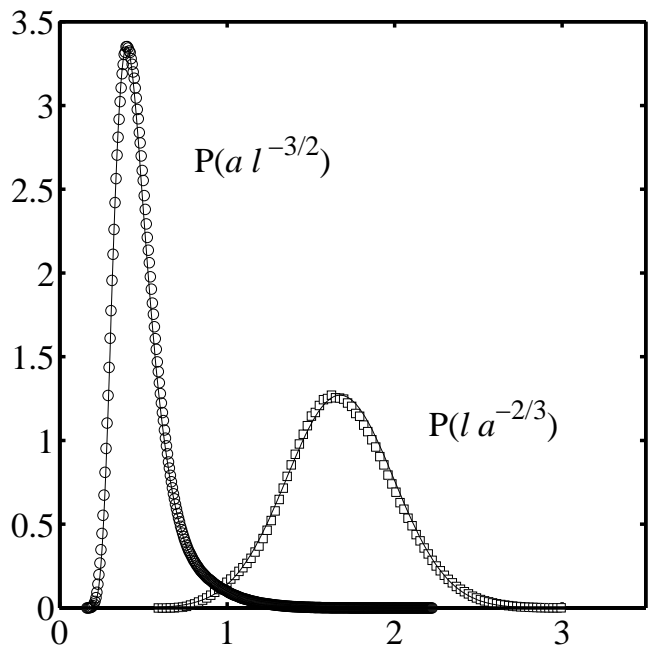


FIG. 3: Cross-Sectional scaling functions of the Hack distribution for the Scheidegger model with lattice constant equal to unity. Both distributions are normalized. The right distribution is for l fixed and a varying and is postulated to be a normal distribution. The left distribution is for a fixed and l varying and is a form of an inverse Gaussian [58]. The data used was obtained for all sites with $l \geq 100$ and $a \geq 500$ respectively. Each distribution was obtained from ten realizations of the Scheidegger model on a $10^4 \times 10^4$ lattice.

We estimate the mean of F_l to be $\theta \simeq 1.675$ (this is the same θ as found in equation (4)) and the standard deviation to be $\eta \simeq 0.321$. The fit is shown in Figure 3 as a solid line. The above equation agrees with the form of the scaling ansatz of equation (5) and we now have the assertion that F_l is a Gaussian defined by the two parameters θ and η .

Note that the θ and η are coefficients for the actual mean and standard deviation. In other words, for fixed a , the mean of $P(l|a)$ is $\theta a^{2/3}$ and its standard deviation is $\eta a^{2/3}$. Having observed their context, we will refer to θ and η as the Hack mean coefficient and Hack standard deviation coefficient.

From this starting point we can create $P(a, l)$ and $P(a|l)$, the latter providing a useful test. Since $P(a) \sim N_a a^{-\tau} = N_a a^{-4/3}$, as per equation (11), we have

$$\begin{aligned} P(a, l) &= \frac{N_a}{a^{4/3}} \frac{1}{\sqrt{2\pi a^{2/3} \eta}} \exp\{-(la^{-2/3} - \theta)^2 / 2\eta^2\}, \\ &= \frac{N_a}{\sqrt{2\pi a^2 \eta}} \exp\{-(la^{-2/3} - \theta)^2 / 2\eta^2\}. \end{aligned} \quad (17)$$

As expected, we observe the form of equation (17) to be

in accordance with that of equation (13). Note that the scaling function F (and equivalently G) is defined by the three parameters θ , η and N_a , the latter of which may be determined in terms of the former as we will show below. Also, since we expect all scaling functions to be only asymptotically correct, we cannot use equation (17) to find an expression for the normalization N_a . Equation (17) ceases to be valid for small a and l . However, we will be able to do so once we have $P(a|l)$ since we are able to presume l is large and therefore that the scaling form is exact. Using equation (15) and the fact that $P(a|l) = P(a, l)/P(l)$ from equation (10) we then have

$$\begin{aligned} P(a|l) &= \frac{\pi l^{3/2}}{2} \frac{N_a}{\sqrt{2\pi a^2 \eta}} \exp\{-(l/a^{2/3} - \theta)^2/2\eta^2\}, \\ &= \frac{N_a \sqrt{\pi} l^{3/2}}{2^{3/2} a^2 \eta} \exp\{-(l/a^{2/3} - \theta)^2/2\eta^2\}, \\ &= \frac{1}{l^{3/2}} \frac{N_a \sqrt{\pi}}{2^{3/2} \eta} (a/l^{3/2})^{-2} \\ &\quad \times \exp\{-((a/l^{3/2})^{-2/3} - \theta)^2/2\eta^2\}. \end{aligned} \quad (18)$$

In rearranging the expression of $P(a|l)$, we have made clear that its form matches that of equation (5).

A closed form expression for the normalization factor N_a may now be determined by employing the fact that $\int_{a=0}^{\infty} da P(a|l) = 1$.

$$\begin{aligned} 1 &= \int_{a=0}^{\infty} da P(a|l), \\ &= \int_{a=0}^{\infty} \frac{da}{l^{3/2}} \frac{N_a \sqrt{\pi}}{2^{3/2} \eta} (a/l^{3/2})^{-2} \\ &\quad \times \exp\{-((a/l^{3/2})^{-2/3} - \theta)^2/2\eta^2\}, \\ &= \frac{N_a \sqrt{3\pi}}{2^{5/2} \eta} \int_{u=0}^{\infty} du u^{1/2} \exp\{-(u - \theta)^2/2\eta^2\}, \end{aligned} \quad (19)$$

where we have used the substitution $a/l^{3/2} = u^{-3/2}$ and hence also $l^{-3/2} da = (-3/2)u^{-5/2} du$. We therefore have

$$N_a = \frac{2^{5/2} \eta}{\sqrt{3\pi}} \left[\int_{u=0}^{\infty} du u^{1/2} \exp\{-(u - \theta)^2/2\eta^2\} \right]^{-1}. \quad (20)$$

We may thus write down all of the scaling functions F_l , F_a , F and G for the Scheidegger model:

$$F_l(z) = \frac{1}{\sqrt{2\pi\eta}} \exp\{-(z - \theta)^2/2\eta^2\}, \quad (21)$$

$$F_a(z) = \frac{N_a \sqrt{\pi}}{2^{3/2} \eta} z^{-2} \exp\{-(z^{-2/3} - \theta)^2/2\eta^2\}, \quad (22)$$

$$F(z) = \frac{N_a}{\sqrt{2\pi\eta}} \exp\{-(z - \theta)^2/2\eta^2\}, \text{ and} \quad (23)$$

$$G(z) = \frac{2N_a}{\sqrt{\pi} 2^{3/2} \eta} z^{-2} \exp\{-(z^{-2/3} - \theta)^2/2\eta^2\}. \quad (24)$$

Recall that all of these forms rest on the assumption that $F_l(z)$ is a Gaussian. In order to check this assumption, we return to Figure 3. The empirical distribution

$P(z = a/l^{3/2})$ is shown on the left marked with circles. The solid line through these points is $F_a(z)$ as given above in equation (21). There is an excellent match so we may be confident about our proposed form for $F_a(z)$. We note that the function $F_a(z)$ may be thought of as a fractional inverse Gaussian distribution, the inverse Gaussian being a well known distribution arising in the study of first passage times for random walks [57]. It is worth contemplating the peculiar form of $P(a|l)$ in terms of first return random walks. Here, we have been able to postulate the functional form of the distribution of areas bound by random walks that first return after n steps. If one could understand the origin of the Gaussian and find analytic expressions for θ and η , then the problem would be fully solved.

VI. AREA-LENGTH DISTRIBUTION EXTENDED TO REAL NETWORKS

We now seek to extend these results for Scheidegger's model to real world networks. We will look for the same functional forms for the Hack distributions that we have found above. The conditional probability distributions pertaining to Hack's law take on the forms

$$P(l|a) = 1/a^{-h} F_l(la^{-h}) = \frac{a^{-h}}{\sqrt{2\pi\eta}} \exp\{-(la^{-h} - \theta)^2/2\eta^2\}, \quad (25)$$

and

$$\begin{aligned} P(a|l) &= l^{-1/h} F_a(al^{-1/h}) \\ &= l^{-1/h} \frac{N_a}{\sqrt{2\pi} N_l \eta} (al^{-1/h})^{-2} \exp\{-((al^{-1/h})^{-h} - \theta)^2/2\eta^2\}, \end{aligned} \quad (26)$$

and the full Hack distribution is given by

$$\begin{aligned} P(a, l) &= a^2 F(la^{-h}) = l^{-2/h} G(al^{-1/h}) \\ &= \frac{N_a}{\sqrt{2\pi\eta} a^2} \exp\{-(la^{-h} - \theta)^2/2\eta^2\}. \end{aligned} \quad (27)$$

with N_a determined by equation (20). The three parameters h , the Hack exponent, θ , the Hack mean coefficient, and η , the Hack standard deviation coefficient, are in principle landscape dependent. Furthermore, in η we have a basic measure of fluctuations in the morphology of basins.

Figures 4 and 5 present Hack scaling functions for the Mississippi and Nile river basins. These Figures is to be compared with the results for the Scheidegger model in Figure 3.

For both rivers, Hack's exponent h was determined first from a stream ordering analysis (we discuss stream ordering later in Section X). Estimates of the parameters θ and η were then made using the scaling function F_l presuming a Gaussian form.

We observe the Gaussian fit for the Mississippi is more satisfactory than that for the Nile. These fits are not

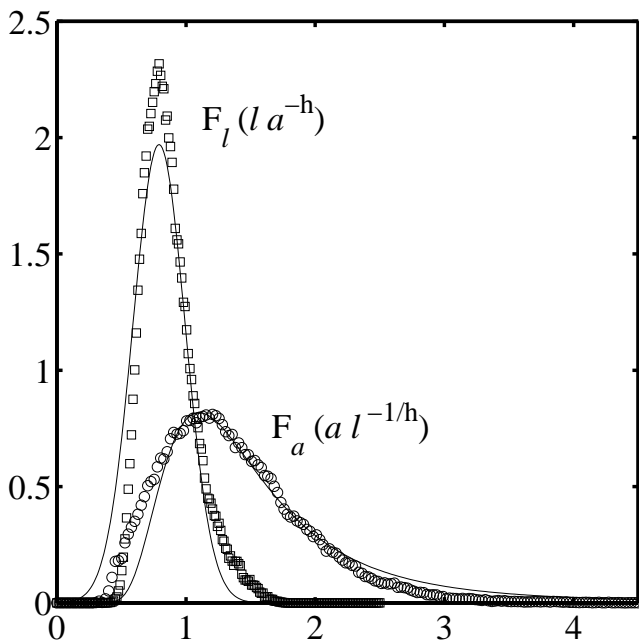


FIG. 4: Cross-sectional scaling functions of the Hack distribution for the Mississippi. The estimates used for Hack’s exponent are $h = 0.55$ and $h = 0.50$ respectively, the determination of which is discussed in section VII. The fits indicated by the smooth curves to the data are made as per the Scheidegger model in Figure 3 and according to equations (25) and (25). The values of the Hack mean coefficient and standard deviation coefficient are estimated to be $\theta \simeq 0.80$ and $\eta \simeq 0.20$.

rigorously made because even though we have chosen data ranges where deviations (which we address in the following section) are minimal, deviations from scaling do still skew the distributions. The specific ranges used to obtain F_l and F_a respectively are for the Mississippi: $8.5 < \log_{10} a < 9.5$ and $4.75 < \log_{10} l < 6$, and for the Nile: $9 < \log_{10} a < 11$ and $5.5 < \log_{10} l < 6$ (areas are in km^2 and lengths km). Furthermore, we observe that the estimate of h has an effect in the resulting forms of F_l and F_a . Nevertheless, here we are attempting to capture the essence of the generalized form of Hack’s law in real networks.

We then use the parameters h , θ and η and equation (26) to construct our theoretical F_a , the smooth curves in Figures 4 and 5. As for the Scheidegger model data in Figure 3, we see in both examples approximate agreement between the measured F_a and the one predicted from the form of F_l . Table I shows estimates of h , θ and η for the five major river basins studied.

Given our reservations about the precision of these values of θ and η , we are nevertheless able to make qualitative distinctions. Recalling that $\langle l \rangle = \theta a^h$, we see that, for fixed h , higher values of θ indicate relatively longer stream lengths for a given area and hence longer and thin-

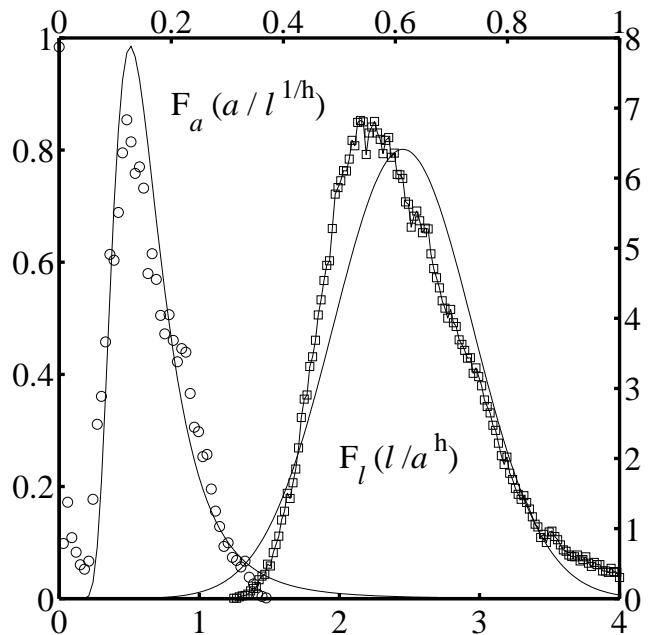


FIG. 5: Cross-sectional scaling functions of the Hack distribution for the Nile. The top and right axes correspond to F_a and the bottom and left to F_l . The Hack exponent used is $h = 0.50$ and the values of the Hack mean coefficient and standard deviation coefficient are estimate to be $\theta \simeq 2.45$ and $\eta \simeq 0.50$ [59].

River network	θ	η	h
Mississippi	0.80	0.20	0.55
Amazon	1.90	0.35	0.52
Nile	2.45	0.50	0.50
Kansas	0.70	0.15	0.57
Congo	0.89	0.18	0.54

TABLE I: Estimates of Hack distribution parameters for real river networks. The scaling exponent h is Hack’s exponent. The parameters θ and η are coefficients of the mean and standard deviation of the conditional probability density function $P(l|a)$ and are fully discussed in the text [60].

ner basins. The results therefore suggest the Nile, and to a lesser degree the Amazon, have basins with thinner profiles than the Congo and, in particular, the Mississippi and Kansas. This seems not unreasonable since the Nile is a strongly directed network constrained within a relatively narrow overall shape. This is somewhat in spite of the fact that the shape of an overall river basin is not necessarily related to its internal basin morphology, an observation we will address later in Section X.

The importance of θ is tempered by the value of h . Hack’s exponent affects not only the absolute measure of

stream length for a given area but also how basin shapes change with increasing area. So, in the case of the Kansas the higher value of h suggests basin profiles thin with increasing size. This is in keeping with overall directness of the network. Note that our measurements of the fractal dimension d of stream lengths for the Kansas place it to be $d = 1.04 \pm 0.02$. Therefore, $d/h \simeq 1.9 < 2$ and elongation is still expected when we factor in the scaling of l with L_{\parallel} .

The Nile and Amazon also all have relatively high η indicating greater fluctuations in basin shape. In comparison, the Mississippi, Kansas and Congo appear to have less variation. Note that the variability of the Kansas is in reasonable agreement with that of the whole Mississippi river network for which it is a sub-basin.

Finally, regardless of the actual form of the distribution underlying Hack's law, fluctuations are always present and an estimate of their extent is an important measurement. Thus, the Hack mean and standard deviation coefficients, θ and η , are suggested to be of sufficient worth so as to be included with any measurement of the Hack exponent h .

VII. DEVIATIONS FROM SCALING

In generalizing Hack's law, we have sought out regions of robust scaling, discarding ranges where deviations become prominent. We now bring our attention to the nature of the deviations themselves.

We observe three major classes of deviations which we will define by the scales at which they occur: small, intermediate and large. Throughout the following sections we primarily consider deviations from the mean version of Hack's law, $\langle l \rangle = \theta a^h$, given in equation (4). Much of the understanding we gain from this will be extendable to deviations for higher moments.

To provide an overview of what follows, examples of mean-Hack distributions for the Kansas river and the Mississippi are shown in Figures 6(a) and 6(b). Hack's law for the Kansas river exhibits a marked deviation for small areas, starting with a near linear relationship between stream length and area. A long crossover region of several orders of magnitude in area then leads to an intermediate scaling regime wherein we attempt to determine the Hack exponent h . In doing so, we show that such regions of robust scaling are surprisingly limited for river network quantities. Moreover, we observe that, where present, scaling is only approximate and that no exact exponents can be ascribed to the networks we study here. It follows that the identification of universality classes based on empirical evidence is a hazardous step.

Finally, the approximate scaling of this intermediate region then gives way to a break down in scaling at larger scales due to low sampling and correlations with basin shape. The same deviations are present in the relatively coarse-grained Mississippi data but are less pronounced.

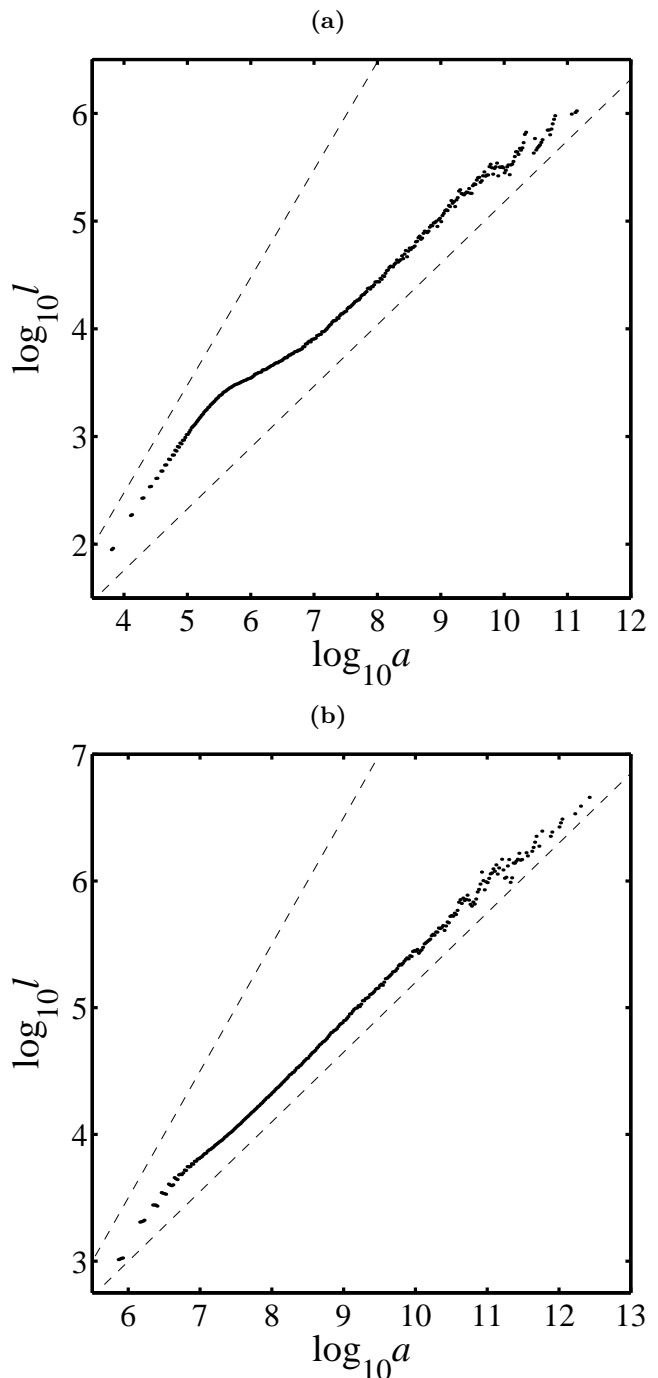


FIG. 6: The mean version of Hack's law for the Kansas, (a), and the Mississippi, (b). The units of lengths and areas are meters and square meters. These are calculated from the full Hack distributions shown in Figures 1(a) and 1(b) by finding $\langle l \rangle$ for each value of basin area a . Area samples are taken every 0.02 orders of magnitude in logarithmic space. The upper dashed lines represent a slope of unity in both plots and the lower lines the Hack exponents 0.57 and 0.55 for the Kansas and Mississippi respectively. For the Kansas, there is a clear deviation for small area which rolls over into a region of very slowly changing derivative before breaking up at large scales. Deviations from scaling are present for the lower resolution dataset of the Mississippi but to a lesser extent.

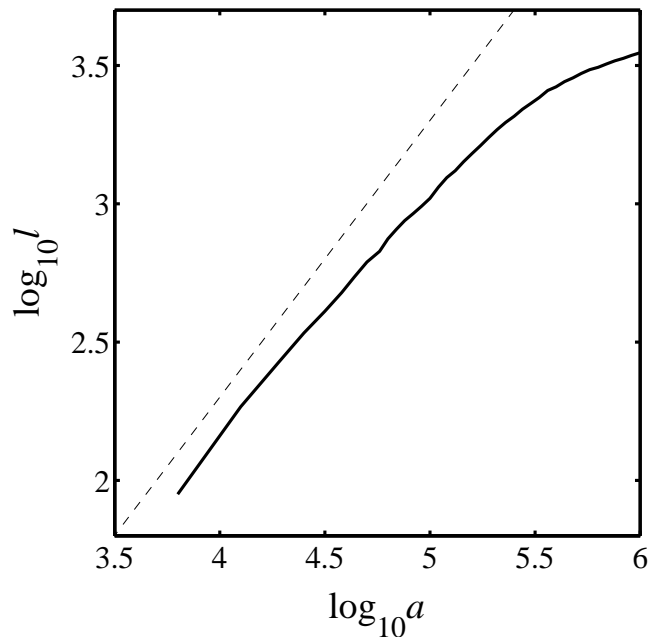


FIG. 7: The linearity of Hack's law at small scales for the Kansas river. The linear regime enters a crossover region after almost 1.5 orders of magnitude in area. This is an expanded detail of the mean Hack's law given in Figure 6(a) and areas and lengths are in square meters and meters.

VIII. DEVIATIONS AT SMALL SCALES

At small scales, we find the mean-Hack distribution to follow a linear relationship, i.e., $l \propto a^1$. This feature is most evident for the Kansas river as shown in Figure 6(a) and in more detail in Figure 7. The linear regime persists for nearly 1.5 orders of magnitude in basin area. To a lesser extent, the same trend is apparent in the Mississippi data, Figure 6(b).

Returning to the full Hack distribution of Figures 1(a) and 1(b), we begin to see the origin of this linear regime. In both instances, a linear branch separates from the body of the main distribution. Since l cannot grow faster than a^1 , the linear branch marks an upper bound on the extent of the distribution in (a, l) coordinates. When averaged to give the mean-Hack distribution, this linear data dominates the result for small scales.

We find this branch evident in all Hack distributions. It is not an artifact of resolution and in fact becomes more pronounced with increased map precision. The origin of this linear branch is simple: data points along the branch correspond to positions in narrow sub-networks, i.e., long, thin "valleys." To understand the separation of this linear branch from the main body of the distribution, consider Figure 8 which depicts a stream draining such a valley with length and area (l_1, a_1) that meets a

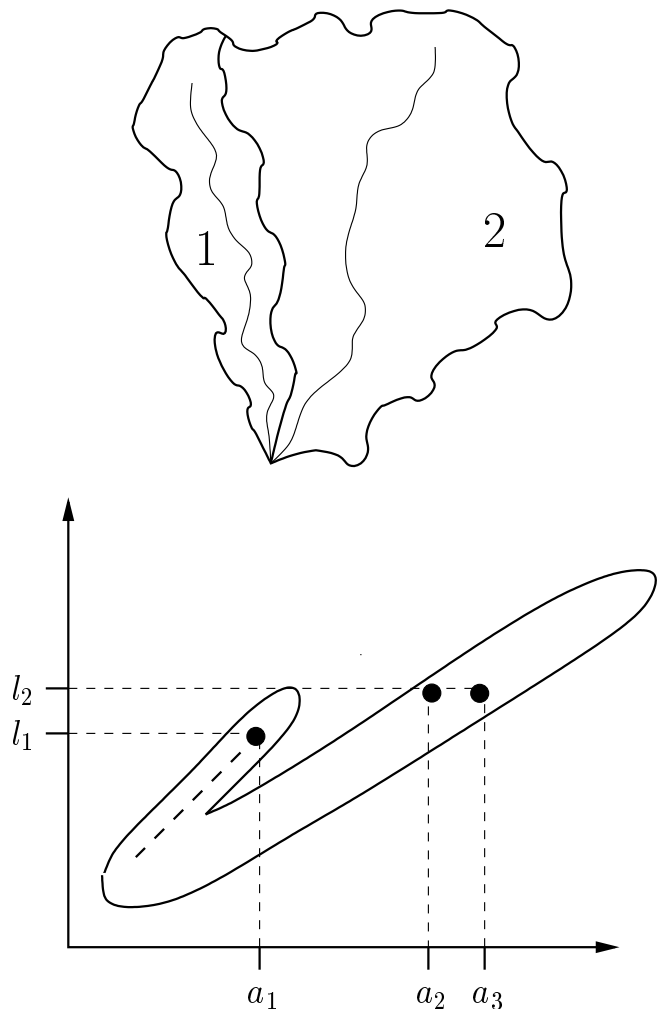


FIG. 8: Origin of the linear branch in the Hack distribution. The sub-basins labeled 1 and 2 depicted on the left have areas a_1 and a_2 and lengths l_1 and l_2 . These sub-basins combine to form a basin of area $a_3 = a_1 + a_2$ and main stream length $l_3 = \max(l_1, l_2) = l_2$. Since sub-basin 1 is a linear sub-network (a valley) the pair (a_1, l_1) lie along the linear branch of the Hack distribution as shown on the right. Points along the main stream of sub-basin 1 lie along the dashed line leading to the coordinate (a_1, l_1) . On combining with the second basin, the jump in the resultant area creates a jump from (a_1, l_1) to (a_3, l_2) in the main body of the Hack distribution.

stream from a basin with characteristics (l_2, a_2) . The area and length of the basin formed at this junction is thus $(a_3, l_3) = (a_1 + a_2, \max(l_1, l_2))$ (in the Figure, $\max(l_1, l_2) = l_2$). The greater jump in area moves the point across into the main body of the Hack distribution, creating the separation of the linear branch.

In fact, the full Hack distribution is itself comprised of many such linear segments. As in the above example,

until a stream does not meet any streams of comparable size, then its area and length will roughly increase in linear fashion. When it does meet such a stream, there is a jump in area and the trace of a new linear segment is started in the distribution. We will see this most clearly later on when we study deviations at large scales.

For very fine scale maps, on the order of meters, we might expect to pick up the scale of the unchannelized, convex regions of a landscape, i.e., “hillslopes” [61]. This length scale represents the typical separation of branches at a network’s finest scale. The computation of stream networks for these hillslope regions would result in largely non-convergent (divergent or parallel) flow. Therefore, we would have linear “basins” that would in theory contribute to the linear branch we observe [10]. Potentially, the crossover in Hack’s law could be used as a determinant of hillslope scale, a crucial parameter in geomorphology [61, 62]. However, when long, thin network structures are present in a network, this hillslope scale is masked by their contribution.

Whether because of the hillslope scale or linear network structure, we see that at small scales, Hack’s law will show a crossover in scaling from $h = 1$ to a lower exponent. The crossover’s position depends on the extent of linear basins in the network. For example, in the Kansas River basin, the crossover occurs when $(l, a) = (4 \times 10^3 \text{m}, 10^7 \text{m}^2)$. Since increased map resolution can only increase measures of length, the crossover’s position must occur at least at such a length scale which may be many orders of magnitude greater than the scale of the map.

However, the measurement of the area of such linear basins will potentially grow with coarse-graining. Note that for the Mississippi mean-Hack distribution, the crossover begins around $a = 10^{6.5} \text{m}^2$ whereas for the Kansas, the crossover initiates near $a = 10^{5.5} \text{m}^2$ but the ends of the crossovers in both cases appear to agree, occurring at around $a = 10^7 \text{m}^2$. Continued coarse-graining will of course eventually destroy all statistics and introduce spurious deviations. Nevertheless, we see here that the deviation which would only be suggested in the Mississippi data is well confirmed in the finer-grain Kansas data.

IX. DEVIATIONS AT INTERMEDIATE SCALES

As basin area increases, we move out of the linear regime, observing a crossover to what would be considered the normal scaling region of Hack’s law. We detail our attempts to measure the Hack exponents for the Kansas and Mississippi examples. Rather than relying solely on a single regression on a mean-Hack distribution, we employ a more precise technique that examines the distribution’s derivative. As we will show, we will not be able to find a definite value for the Hack exponent in either case, an important result in our efforts to deter-

mine whether or not river networks belong to specific universality classes.

To determine h , we consider Hack’s law (equation (4)) explicitly in logarithmic coordinates,

$$\log_{10} \langle l(a) \rangle = \log_{10} \theta + h \log_{10} a. \quad (28)$$

The derivative of this equation with respect to $\log_{10} a$ then gives Hack’s exponent as a function of area,

$$h(a) = \frac{d}{d \log_{10} a} \log_{10} \langle l(a) \rangle. \quad (29)$$

We may think of $h(a)$ as a “local Hack exponent.” Note that non-constant trends in $h(a)$ indicate scaling does not hold. We calculate the discrete derivative as above for the Kansas and Mississippi. We smooth the data by taking running averages with varying window sizes of n samples, the results for $n = 32$ being shown in Figures 9(a) and 9(b) where the spacing of $\log a$ is 0.02 orders of magnitude. Thus, the running averages for the figures are taken over corresponding area ranges 0.64 orders of magnitude.

Now, if the scaling law in question is truly a scaling law, the above type of derivative will fluctuate around a constant value of exponent over several orders of magnitude. With increasing n , these fluctuations will necessarily decrease and we should see the derivative holding steady around the exponent’s value.

At first glance, we notice considerable variation in $h(a)$ for both data sets with the Kansas standing out. Fluctuations are reduced with increasing n but we observe continuous variation of the local Hack exponent with area. For the example of the Kansas, the linear regime and ensuing crossover appear as a steep rise followed by a drop and then another rise during all of which the local Hack exponent moves well below 1/2.

It is after these small scale fluctuations that we would expect to find Hack’s exponent. For the Kansas river data, we see the derivative gradually climbs for all values of n before reaching the end of the intermediate regime where the putative scaling breaks down altogether.

For the Kansas show in Figure 9(a), the dashed line represents $h = 0.57$, our estimate of Hack’s exponent from simple regression on the mean-Hack distribution of Figure 6(a). For the regression calculation, the intermediate region was identified from the figure to be $10^7 < a < 10^{10} \text{m}^2$. We see from the smoothed derivative in Figure 9(a) that the value $h = 0.57$ is not precise. After the crossover from the linear region has been completed, we observe a slow rise from $h \simeq 0.54$ to $h \simeq 0.63$. Thus, the local Hack exponent $h(a)$ gradually climbs above $h = 0.57$ rather than fluctuate around it.

A similar slow change in $h(a)$ is observed for the Mississippi data. We see in Figure 9(b) a gradual rise and then fall in $h(a)$. The dashed line here represents $h = 0.55$, the value of which was determined from Figure 6(b) using regression on the range $10^9 < a < 10^{11.5} \text{m}^2$. The range of $h(a)$ is roughly $[0.52, 0.58]$. Again, while $h = 0.55$

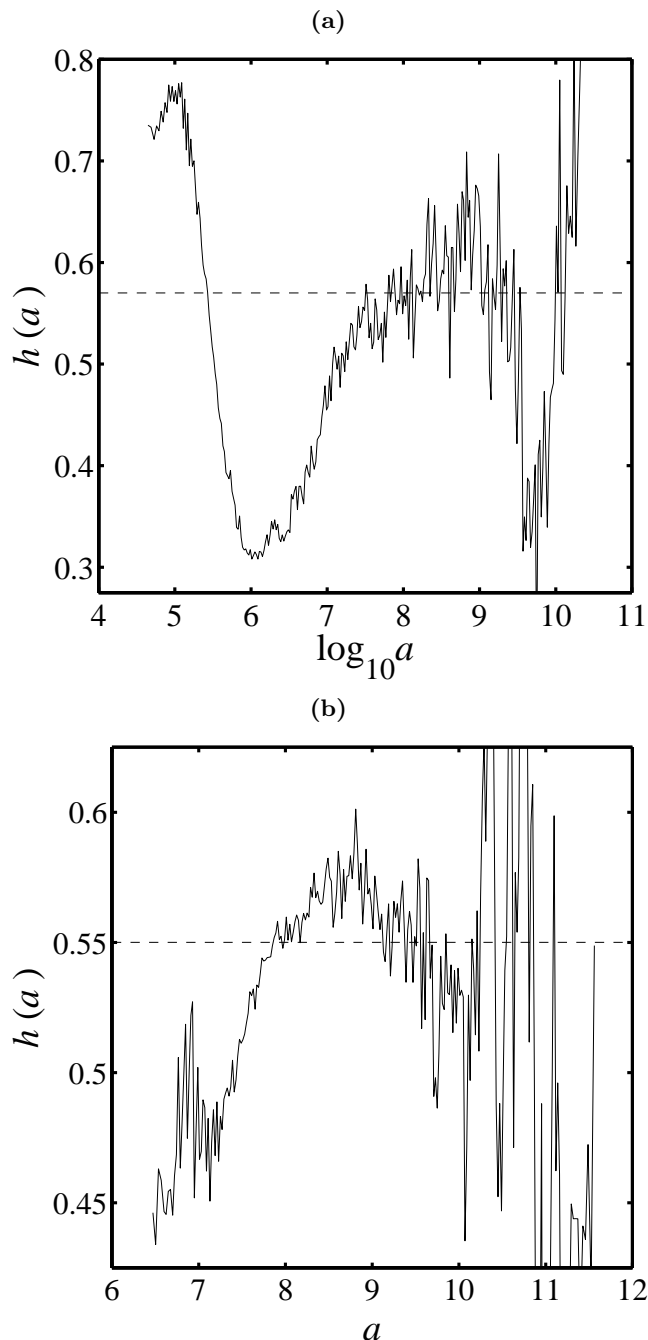


FIG. 9: Variation in Hack's exponent for the Kansas, (a), and the Mississippi, (b). The area a is in m^2 . The plots are derivatives of the mean-Hack distributions given in Figures 6(a) and 6(b). Both derivatives have been smoothed by taking running averages over 0.64 orders of magnitude in a . For the Kansas, the dashed line is set at $h = 0.57$, Hack's exponent estimated via simple regression analysis for points with $10^7 < a < 10^{10} \text{ m}^2$. The local exponent is seen to gradually rise through the $h = 0.57$ level indicating scaling is not robust. For the Mississippi in (b), the dashed line is a Hack exponent of 0.55 calculated from regression on data in the interval $10^9 < a < 10^{11.5} \text{ m}^2$. The local Hack exponent is seen to gradually rise and fall about this value.

approximates the derivative throughout this intermediate range of Hack's law, we cannot claim it to be a precise value.

We observe the same drifts in $h(a)$ in other datasets and for varying window size n of the running average. The results suggest that we cannot assign specific Hack exponents to these river networks and are therefore unable to even consider what might be an appropriate universality class. The value of h obtained by regression analysis is clearly sensitive to the range of a used. Furthermore, these results indicate that we should maintain healthy reservations about the exact values of other reported exponents.

X. DEVIATIONS AT LARGE SCALES

We turn now to deviations from Hack's law at large scales. As we move beyond the intermediate region of approximate scaling, fluctuations in $h(a)$ begin to grow rapidly. This is clear on inspection of the derivatives of Hack's law in Figures 9(a) and 9(b). There are two main factors conspiring to drive these fluctuations up. The first is that the number of samples of sub-basins with area a decays algebraically in a . This is just the observation that $P(a) \propto a^{-\tau}$ as per equation (11). The second factor is that fluctuations in l and a are on the order of the parameters themselves. This follows from our generalization of Hack's law which shows, for example, that the moments $\langle l^q \rangle$ of $P(l|a)$ grow like a^{qh} . Thus, the standard deviation grows like the mean: $\sigma(l) = (\langle l^2 \rangle - \langle l \rangle^2)^{1/2} \propto a^h \propto \langle l \rangle$.

A Stream ordering and Horton's laws

So as to understand these large scale deviations from Hack's law, we need to examine network structure in depth. One way to do this is by using Horton-Strahler stream ordering [38, 63] and a generalization of the well-known Horton's laws [38, 64, 65, 39, 36]. This will naturally allow us to deal with the discrete nature of a network that is most apparent at large scales.

Stream ordering discretizes a network into a set of stream segments (or, equivalently, a set of nested basins) by an iterative pruning. Source streams (i.e., those without tributaries) are designated as stream segments of order $\omega = 1$. These are removed from the network and the new source streams are then labelled as order $\omega = 2$ stream segments. The process is repeated until a single stream segment of order $\omega = \Omega$ is left and the basin itself is defined to be of order Ω .

Natural metrics for an ordered river network are n_ω , the number of order ω stream segments (or basins), \bar{a}_ω , the average area of order ω basins, \bar{l}_ω , the average main stream length of order ω basins, and $\bar{l}_\omega^{(s)}$, the average length of order ω stream segments. Horton's laws

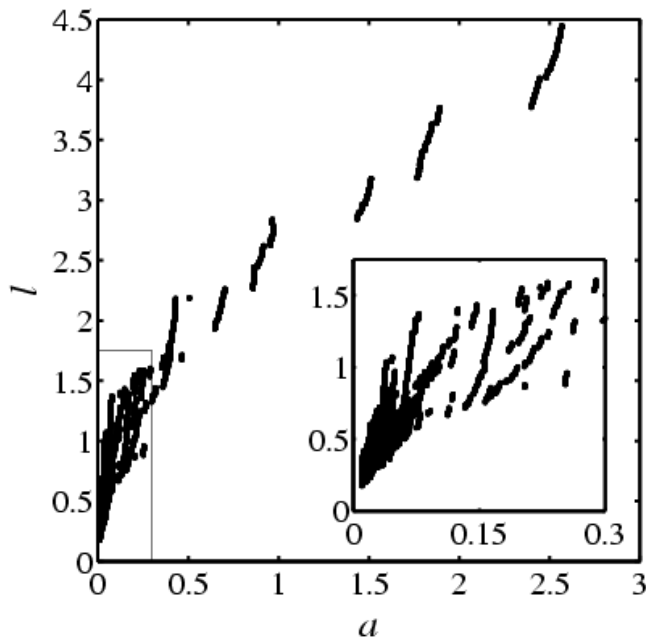


FIG. 10: Hack distribution for the Mississippi plotted in linear space. The area units a is 10^{12} m² and length l is 10^6 m. The discreteness of the basin structure is clearly indicated by the isolated, linear fragments. The inset is a blow-up of the box on the main graph.

state that these quantities change regularly from order to order, i.e.,

$$\frac{n_\omega}{n_{\omega+1}} = R_n \quad \text{and} \quad \frac{\bar{X}_{\omega+1}}{\bar{X}_\omega} = R_X, \quad (30)$$

where $X = a, l$ or $l^{(s)}$. Note that all ratios are defined to be greater than unity since areas and lengths increase but number decreases. Also, there are only two independent ratios since $R_a \equiv R_n$ and $R_l \equiv R_{l^{(s)}}$ [39]. Horton's laws mean that stream-order quantities change exponentially with order. For example, (30) gives that $l_\omega \propto (R_l)^\omega$.

B Discrete version of Hack's law

Returning to Hack's law, we examine its large scale fluctuations with the help of stream ordering. We are interested in the size of these fluctuations and also how they might correlate with the overall shape of a basin. First, we note that the structure of the network at large scales is explicitly discrete. Figure 10 demonstrates this by plotting the distribution of (a, l) without the usual logarithmic transformation. Hack's law is seen to be composed of linear fragments. As explained above in Figure 8, areas and length increase in proportion to each other along streams where no major tributaries enter. As

soon as a stream does combine with a comparable one, a jump in drainage area occurs. Thus, we see in Figure 10 isolated linear segments which upon ending at a point (a_1, l_1) begin again at $(a_1 + a_2, l_1)$, i.e., the main stream length stays the same but the area is shifted.

We consider a stream ordering version of Hack's law given by the points $(\bar{a}_\omega, \bar{l}_\omega)$. The scaling of these data points is equivalent to scaling in the usual Hack's law. Also, given Horton's laws, it follows that $h = \ln R_l / \ln R_n$ (using $R_a \equiv R_n$). Along the lines of the derivative we introduced to study intermediate scale fluctuations in equation (29), we have here an order-based difference:

$$h_{\omega, \omega-1} = \frac{\log \bar{l}_\omega / \bar{l}_{\omega-1}}{\log \bar{a}_\omega / \bar{a}_{\omega-1}}. \quad (31)$$

We can further extend this definition to differences between non-adjacent orders:

$$h_{\omega, \omega'} = \frac{\log \bar{l}_\omega / \bar{l}_{\omega'}}{\log \bar{a}_\omega / \bar{a}_{\omega'}}. \quad (32)$$

This type of difference, where $\omega' < \omega$, may be best thought of as a measure of trends rather than an approximate discrete derivative.

Using these discrete differences, we examine two features of the order-based versions of Hack's law. First we consider correlations between large scale deviations within an individual basin and second, correlations between overall deviations and basin shape. For the latter, we will also consider deviations as they move back into the intermediate scale. This will help to explain the gradual deviations from scaling we have observed at intermediate scales.

Since deviations at large scales are reflective of only a few basins, we require an ensemble of basins to provide sufficient statistics. As an example of such an ensemble, we take the set of order $\Omega = 7$ basins of the Mississippi basin. For the dataset used here where the overall basin itself is of order $\Omega = 11$, we have 104 order $\Omega = 7$ sub-basins. The Horton averages for these basins are $\bar{a}_7 \simeq 16600$ km², $\bar{l}_7 \simeq 350$ km, and $\bar{L}_7 \simeq 210$ km.

For each basin, we first calculate the Horton averages $(\bar{a}_\omega, \bar{l}_\omega)$. We then compute $h_{\omega, \omega-1}$, the Hack difference given in equation (31). To give a rough picture of what is observed, Figure 11 shows a scatter plot of $h_{\omega, \omega-1}$ for all order $\Omega = 7$ basins. Note the increase in fluctuations with increasing ω . This increase is qualitatively consistent with the smooth versions found in the single basin examples of Figures 9(a) and 9(b). In part, less self-averaging for larger ω results in a greater spread in this discrete derivative. However, as we will show, these fluctuations are also correlated with fluctuations in basin shape.

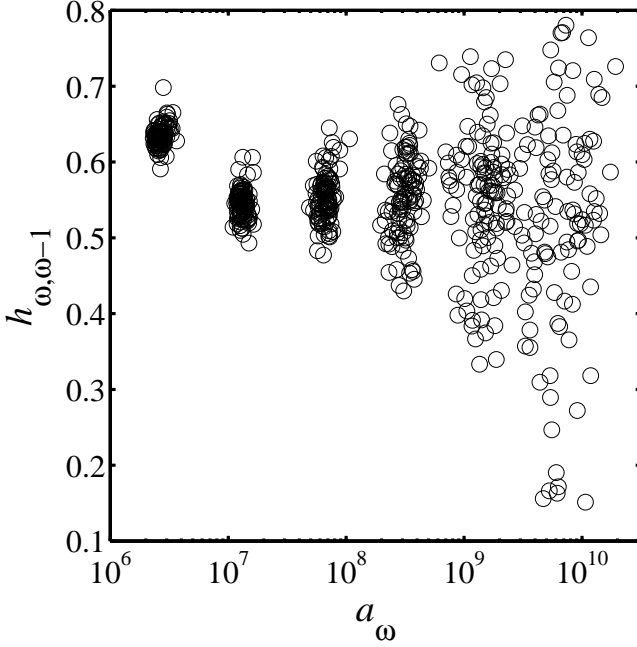


FIG. 11: Differences of the stream order-based version of Hack’s law for 104 order $\Omega = 7$ basins of the Mississippi (compare the continuous versions given in Figure 9) The plots are overlaid to give a sense of the increase in fluctuations of the local Hack exponent $h_{\omega, \omega-1}$ with increasing order ω . The clusters correspond to $\omega = 1, 2, \dots, 7$, moving across from left to right.

C Effect of basin shape on Hack’s law

In what follows, we extract two statistical measures of correlations between deviations in Hack’s law and overall basin shape. These are r , the standard linear correlation coefficient and r_s , the Spearman rank-order correlation coefficient [66, 67, 68]. For N observations of data pairs (u_i, v_i) , r is defined to be

$$r = \frac{\sum_{i=1}^N (u_i - \mu_u)(v_i - \mu_v)}{\sum_{i=1}^N (x_i - \mu_u)^2 \sum_{i=1}^N (y_i - \mu_v)^2} = \frac{C(u, v)}{\sigma_u \sigma_v}, \quad (33)$$

where $C(u, v)$ is the covariance of the u_i ’s and v_i ’s, μ_u and μ_v their means, and σ_u and σ_v their standard deviations. The value of Spearman’s r_s is determined in the same way but for the u_i and v_i replaced by their ranks. From r_s , we determine a two-sided significance p_s via Student’s t -distribution [66].

We define κ , a measure of basin aspect ratio, as

$$\kappa = L^2/a. \quad (34)$$

Long and narrow basins correspond to $\kappa \gg 1$ while for short and wide basins, we have $\kappa \ll 1$

We now examine the discrete derivatives of Hack’s law in more detail. In order to discern correlations

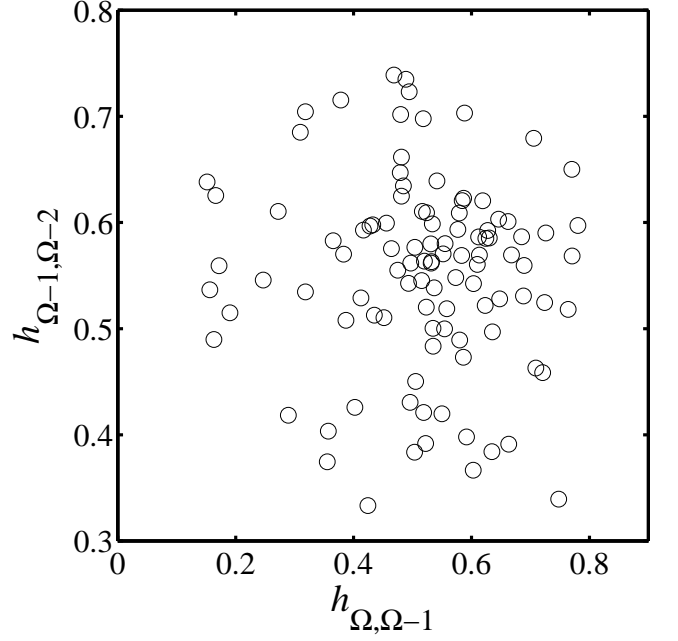


FIG. 12: A comparison of the stream order Hack derivatives $h_{\Omega, \Omega-1}$ and $h_{\Omega-1, \Omega-2}$ for each of the 104 order $\Omega = 7$ basins of the Mississippi. The linear correlation coefficient is $r = -0.06$ and the Spearman correlation coefficient is $r_s = -0.08$. The latter has probability $p_s = 0.43$ indicating there are no significant correlations.

between large scale fluctuations within individual basins, we specifically look at the last two differences in a basin: $h_{\Omega, \Omega-1}$ and $h_{\Omega-1, \Omega-2}$. For each of the Mississippi’s 104 order $\Omega = 7$ basins, these values are plotted against each other in Figure 12. Both our correlation measurements strongly suggest these differences are uncorrelated. The linear correlation coefficient is $r = -0.06 \simeq 0$ and, similarly, we have $r_s = -0.08 \simeq 0$. The significance $p_s = 0.43$ implies that the null hypothesis of uncorrelated data cannot be rejected.

Thus, for Hack’s law in an individual basin, large scale fluctuations are seen to be uncorrelated. However, correlations between these fluctuations and other factors may still exist. This leads us to our second test which concerns the relationship between trends in Hack’s law and overall basin shape.

Figure 13 shows a comparison of the aspect ratio κ and $h_{7,5}$ for the order $\Omega = 7$ basins of the Mississippi. The measured correlation coefficients are $r = 0.50$ and $r_s = 0.53$, giving a significance of $p_s < 10^{-8}$. Furthermore, we find the differences $h_{7,6}$ ($r = 0.34$, $r_s = 0.39$ and $p_s < 10^{-4}$) and $h_{6,5}$ ($r = 0.35$, $r_s = 0.34$ and $p_s < 10^{-3}$) are individually correlated with basin shape. We observe this correlation between basin shape and trends in Hack’s law at large scales, namely $h_{\Omega, \Omega-1}$, $h_{\Omega-1, \Omega-2}$ and $h_{\Omega, \Omega-2}$, repeatedly in our other data sets. In some cases, correlations extend further to $h_{\Omega-2, \Omega-3}$.

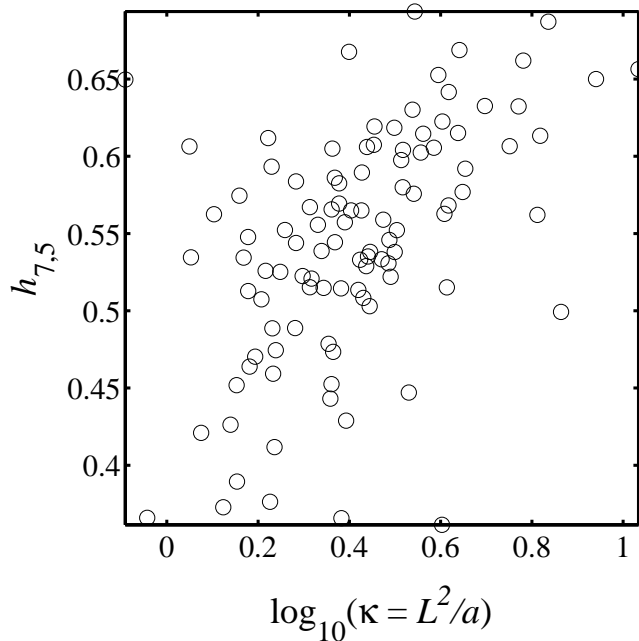


FIG. 13: Correlation between trends in Hack's law and the aspect ratio of a basin as estimated by $\kappa = L^2/a$. The data is for the order $\Omega = 7$ basins of the Mississippi and the specific trend is $h_{7,5}$. The correlation measurements give $r = 0.50$, $r_s = 0.53$ and $p_s < 10^{-8}$.

Since the area ratio R_a is typically in the range 4–5, Hack's law is affected by boundary conditions set by the geometry of the overall basin down to sub-basins one to two orders of magnitude smaller in area than the overall basin. These deviations are present regardless of the absolute size of the overall basin. Furthermore, the origin of the basin boundaries being geologic or chance or both is irrelevant—large scale deviations will still occur. However, it is reasonable to suggest that particularly strong deviations are more likely the result of geologic structure rather than simple fluctuations.

XI. CONCLUSION

Hack's law is a central relation in the study of river networks and branching networks in general. We have shown Hack's law to have a more complicated structure than is typically given attention. The starting generalization is to consider fluctuations around scaling. Using the directed, random network model, a form for the Hack distribution underlying Hack's law may be postulated and reasonable agreement with real networks is observed. Questions of the validity of the distribution aside, the Hack mean coefficient θ and the Hack standard deviation coefficient η should be standard measurements because they provide further points of comparison between theory and

other basins.

With the idealized Hack distribution proposed, we may begin to understand deviations from its form. As with any scaling law pertaining to a physical system, cutoffs in scaling must exist and need to be understood. For small scales, we have identified the presence of linear sub-basins as the source of an initial linear relation between area and stream length. At large scales, statistical fluctuations and geologic boundaries give rise to basins whose overall shape produces deviations in Hack's laws. Both deviations extend over a considerable range of areas as do the crossovers which link them to the region of intermediate scales, particularly the crossover from small scales.

Finally, by focusing in detail on a few large-scale examples networks, we have found evidence that river networks do not belong to well defined universality classes. The relationship between basin area and stream length may be approximately, and in some cases very well, described by scaling laws but not exactly so. The gradual drift in exponents we observe suggests a more complicated picture, one where subtle correlations between basin shape and geologic features are intrinsic to river network structure.

ACKNOWLEDGEMENTS

This work was supported in part by NSF grant EAR-9706220 and the Department of Energy grant DE FG02-99ER 15004.

REFERENCES

- † Author to whom correspondence should be addressed; Electronic address: dodds@segovia.mit.edu; URL: <http://segovia.mit.edu/>
- ‡ Electronic address: dan@segovia.mit.edu
- [1] R. Albert, H. Jeong, and A.-L. Barabasi, *Nature* **401**(6749), 130 (1999).
 - [2] D. J. Watts and S. J. Strogatz, *Nature* **393**, 440 (1998).
 - [3] M. Zamir, *J. Theor. Biol.* **197**, 517 (1999).
 - [4] S. N. Coppersmith, C.-h. Liu, S. Majumdar, O. Narayan, and T. A. Witten, *Phys. Rev. E* **53**(5), 4673 (1996).
 - [5] C. Cherniak, M. Changizi, and D. Kang, *Phys. Rev. E* **59**(5) (1999).
 - [6] B. B. Mandelbrot, *The Fractal Geometry of Nature* (Freeman, San Francisco, 1983).
 - [7] I. Rodríguez-Iturbe and A. Rinaldo, *Fractal River Basins: Chance and Self-Organization* (Cambridge University Press, Great Britain, 1997).
 - [8] A. Rinaldo, I. Rodríguez-Iturbe, and R. Rigon, *Annu. Rev. Earth Planet. Sci* **26**, 289 (1998).
 - [9] P. Ball, *The Self-Made Tapestry* (Oxford, UK, 1998).

- [10] P. S. Dodds and D. H. Rothman, *Annu. Rev. Earth Planet. Sci.* **28**, 571 (2000).
- [11] J. T. Hack, *U.S. Geol. Surv. Prof. Pap.* **294-B**, 45 (1957).
- [12] A. Maritan, A. Rinaldo, R. Rigon, A. Giacometti, and I. Rodríguez-Iturbe, *Phys. Rev. E* **53**(2), 1510 (1996).
- [13] R. Rigon, I. Rodríguez-Iturbe, A. Maritan, A. Giacometti, D. G. Tarboton, and A. Rinaldo, *Water Resour. Res.* **32**(11), 3367 (1996).
- [14] H. Jaeger, S. Nagel, and R. Behringer, *Rev. Mod. Phys.* **68**(4), 1259 (1996).
- [15] L. Kadanoff, *Rev. Mod. Phys.* **71**(1), 435 (1999).
- [16] T. R. Smith and F. P. Bretherton, *Water Resour. Res.* **3**(6), 1506 (1972).
- [17] S. Kramer and M. Marder, *Phys. Rev. Lett.* **68**(2), 205 (1992).
- [18] N. Izumi and G. Parker, *Journal of Fluid Mechanics* **283**, 341 (1995).
- [19] K. Sinclair and R. C. Ball, *Phys. Rev. Lett.* **76**(18), 3360 (1996).
- [20] J. R. Banavar, F. Colaiori, A. Flammini, A. Giacometti, A. Maritan, and A. Rinaldo, *Phys. Rev. Lett.* **78**, 4522 (1997).
- [21] E. Somfai and L. M. Sander, *Phys. Rev. E* **56**(1), R5 (1997).
- [22] R. Pastor-Satorras and D. H. Rothman, *Phys. Rev. Lett.* **80**(19), 4349 (1998).
- [23] R. Pastor-Satorras and D. H. Rothman, *J. Stat. Phys.* **93**, 477 (1998).
- [24] M. Cieplak, A. Giacometti, A. Maritan, A. Rinaldo, I. Rodríguez-Iturbe, and J. R. Banavar, *J. Stat. Phys.* **91**(1/2), 1 (1998).
- [25] A. Giacometti, *Local minimal energy landscapes in river networks* (2000), preprint.
- [26] H. Takayasu and H. Inaoka, *Phys. Rev. Lett.* **68**(7), 966 (1992).
- [27] R. L. Leheny, *Phys. Rev. E* **52**(5), 5610 (1995).
- [28] G. Caldarelli, A. Giacometti, A. Maritan, I. Rodríguez-Iturbe, and A. Rinaldo, *Phys. Rev. E* **55**(5), 4865 (1997).
- [29] C. P. Stark, *Nature* **352**, 405 (1991).
- [30] T. Sun, P. Meakin, and T. Jøssang, *Phys. Rev. E* **49**(6), 4865 (1994).
- [31] T. Sun, P. Meakin, and T. Jøssang, *Phys. Rev. E* **51**(6), 5353 (1995).
- [32] L. B. Leopold and W. B. Langbein, *U.S. Geol. Surv. Prof. Pap.* **500-A**, 1 (1962).
- [33] A. E. Scheidegger, *Bull. Int. Assoc. Sci. Hydrol.* **12**(1), 15 (1967).
- [34] S. S. Manna and B. Subramanian, *Phys. Rev. Lett.* **76**(18), 3460 (1996).
- [35] A. Maritan, F. Colaiori, A. Flammini, M. Cieplak, and J. R. Banavar, *Science* **272**, 984 (1996).
- [36] P. S. Dodds and D. H. Rothman, *Geometry of River Networks II: Distributions of Component Size and Number* (2000), submitted to PRE.
- [37] P. S. Dodds and D. H. Rothman, *Geometry of River Networks III: Characterization of Component Connectivity* (2000), submitted to PRE.
- [38] R. E. Horton, *Bull. Geol. Soc. Am* **56**(3), 275 (1945).
- [39] P. S. Dodds and D. H. Rothman, *Phys. Rev. E* **59**(5), 4865 (1999), cond-mat/9808244.
- [40] E. Tokunaga, *Geophys. Bull. Hokkaido Univ.* **15**, 1 (1966).
- [41] E. Tokunaga, *Geogr. Rep., Tokyo Metrop. Univ.* **13**, 1 (1978).
- [42] E. Tokunaga, *Trans. Jpn. Geomorphol. Union* **5**(2), 71 (1984).
- [43] D. M. Gray, *J. Geophys. Res.* **66**(4), 1215 (1961).
- [44] J. E. Mueller, *Geological Society of America Bulletin* **83**, 3471 (1972).
- [45] M. P. Mosley and R. S. Parker, *Geological Society of America Bulletin* **84**, 3123 (1973).
- [46] J. E. Mueller, *Geological Society of America Bulletin* **84**, 3127 (1973).
- [47] D. R. Montgomery and W. E. Dietrich, *Science* **255**, 826 (1992).
- [48] R. Rigon, I. Rodríguez-Iturbe, and A. Rinaldo, *Water Resour. Res.* **34**(11), 3181 (1998).
- [49] The topography used to extract areas and stream lengths is a composite of United States Geological Survey three-arc-second digital elevation models available on the Internet at www.usgs.gov. These datasets provide grids of elevation data with horizontal resolution on the order of 90 meters. The Kansas river was analyzed directly from the data while the Mississippi basin was studied on a coarse-grained version with horizontal resolution of approximately 1000 meters.
- [50] D. G. Tarboton, R. L. Bras, and I. Rodríguez-Iturbe, *Water Resour. Res.* **26**(9), 2243 (1990).
- [51] H. Takayasu, I. Nishikawa, and H. Tasaki, *Phys. Rev. A* **37**(8), 3110 (1988).
- [52] P. Meakin, J. Feder, and T. Jøssang, *Physica A* **176**, 409 (1991).
- [53] G. Huber, *Physica A* **170**, 463 (1991).
- [54] D. Dhar and S. N. Majumdar, *J. Phys. A: Math. Gen.* **23**, 4333 (1990).
- [55] D. Dhar, *Physica A* **186**, 82 (1992).
- [56] D. Dhar, *Physica A* **263**, 4 (1999).
- [57] W. Feller, *An Introduction to Probability Theory and Its Applications*, vol. I (John Wiley & Sons, New York, 1968), third ed.
- [58] W. Feller, *An Introduction to Probability Theory and Its Applications*, vol. II (John Wiley & Sons, New York, 1968), third ed.
- [59] The data for the Nile and Congo was obtained from the United States Geological Survey's 30-arc-second Hydro1K dataset which may be accessed on the Internet at edcftp.cr.usgs.gov. Note that these Hydro1K datasets have undergone the extra processing of projection onto a uniform grid.
- [60] The dataset used for the Amazon has a horizontal resolution of approximately 1000 meters and comes from 30 arc second terrain data provided by the

- National Imagery and Mapping Agency available on the Internet at www.nima.mil.
- [61] W. Dietrich and D. Montgomery, in *Scale Dependence and Scale Invariance in Hydrology*, edited by G. Sposito (Cambridge University Press, Cambridge, United Kingdom, 1998), pp. 30–60.
- [62] W. E. Dietrich and T. Dunne, in *Channel Network Hydrology*, edited by K. Beven and M. Kirkby (John Wiley & Sons Ltd, New York, 1993), chap. 7, pp. 175–219.
- [63] A. N. Strahler, *EOS Trans. AGU* **38**(6), 913 (1957).
- [64] S. A. Schumm, *Bull. Geol. Soc. Am* **67**, 597 (1956).
- [65] S. Peckham and V. Gupta, *Water Resour. Res.* **35**(9), 2763 (1999).
- [66] W. H. Press, S. A. Teukolsky, W. T. Vetterling, and B. P. Flannery, *Numerical Recipes in C* (Cambridge University Press, 1992), second ed.
- [67] E. L. Lehman, *Nonparametrics : statistical methods based on ranks* (Holden-Day, San Francisco, 1975).
- [68] P. Sprent, *Applied Nonparametric Statistical Methods* (Chapman & Hall, New York, 1993), second ed.